Identification of Novel TSH Interaction Sites by Systematic Binding Analysis of the TSHR Hinge Region

Sandra Mueller, Mariusz W. Szkudlinski, Jörg Schaarschmidt, Robert Günther, Ralf Paschke*, and Holger Jaeschke

Division of Endocrinology and Nephrology (S.M., J.S., R.P., H.J.), and the Institute of Biochemistry (R.G.), University of Leipzig, D-04103 Leipzig, Germany; and Trophogen, Inc. (M.W.S.), Rockville, Maryland 20850

In which ways the binding of the thyroid stimulating hormone to the extracellular domain of its receptor leads to activation of the thyroid-stimulating hormone receptor (TSHR) is currently only incompletely understood. It is known that TSH binding to the TSHR depends on the interaction with the leucine-rich repeat and sulfation at Y385 of the hinge region. Recently it was also shown that electrostatic interactions between positive charges of bovine (b) TSH and the residues E297, E303, and D382 of the hinge region contribute to hormone-TSHR binding. After the identification of these first TSH binding sites in the hinge region, it was apparent that multiple positions in this region remained to be characterized for their roles in hormone binding. The goal of this study was therefore to clarify whether further contact points of TSH exist in the structurally undefined hinge region. Therefore, we systematically analyzed 41 uncharacterized residues of the TSHR hinge region as single mutants regarding differences between cell surface expression and bTSH binding. Indeed, we identified further amino acids of the hinge region with influence on bTSH binding. Some of these contribute to a new binding domain from human TSHR position F381 to D386. These hinge mutants with influence on bTSH binding were also analyzed for binding of the superagonistic human TSH analog TR1401 demonstrating that these positions also have an impact on TR1401 binding. Moreover, side chain variations revealed that different amino acid properties like the negative charge, aromatic as well as hydrophilic characteristics, contribute to maintain the hormone-TSHR hinge interaction. **(*Endocrinology* 152: 3268–3278, 2011)**

The initial step for the activation of the thyroid-stimulating hormone receptor (TSHR) is the binding of the native ligand, the TSH, to the ectodomain of the receptor. The TSHR ecdodomain can be subdivided into the leucine-rich repeat (LRR) and the hinge region (HinR), which links the LRR with the serpentine domain (Fig. 1). There are different descriptions of the length of the HinR sequence (1) because the exact junction between the LRR and the HinR remains unknown. Based on the likely C-terminal extension of the LRR from L260 to Y279 (1), we assumed that P280-D410 constitute the HinR containing the cleavable C-peptide from A317 to G367 (1–3).

It is known that bovine TSH (bTSH) binding to the human TSHR is mediated by the LRR (4, 5) and the sulfation site Y385 (6) as well as the recently identified E297, E303, and D382 of the HinR, which interact with positive charges in the α-loop 1 (α-L1) of bTSH (7, 8). However, the hormone-TSHR binding mechanisms are only incompletely known mainly due to the lack of structural data for the HinR despite elucidation of the binding arrangements between the human FSH and the homologous hormone binding LRR of the FSH receptor by x-ray analysis (9). Moreover, a crystal structure of the corresponding LRR of the TSHR in complex with a thyroid-stimulating autoan-

ISSN Print 0013-7227 ISSN Online 1945-7170
Printed in U.S.A.

doi: 10.1210/en.2011-0153 Received February 10, 2011. Accepted May 4, 2011.
First Published Online May 31, 2011

Abbreviations: α-L1, α-Loop 1; b, bovine; Bmax, maximal bTSH binding; CG, choriogonadotropin; FACS, fluorescence-activated cell sorting; FSHR, FSH receptor; GPH, glycoprotein hormone; GPHR, GPH receptor; h, human; HinR, hinge region; Kd, dissociation constant; LH/CGR, LH/CG receptor; LRR, leucine-rich repeat; TSHR, TSH receptor; wt, wild type.

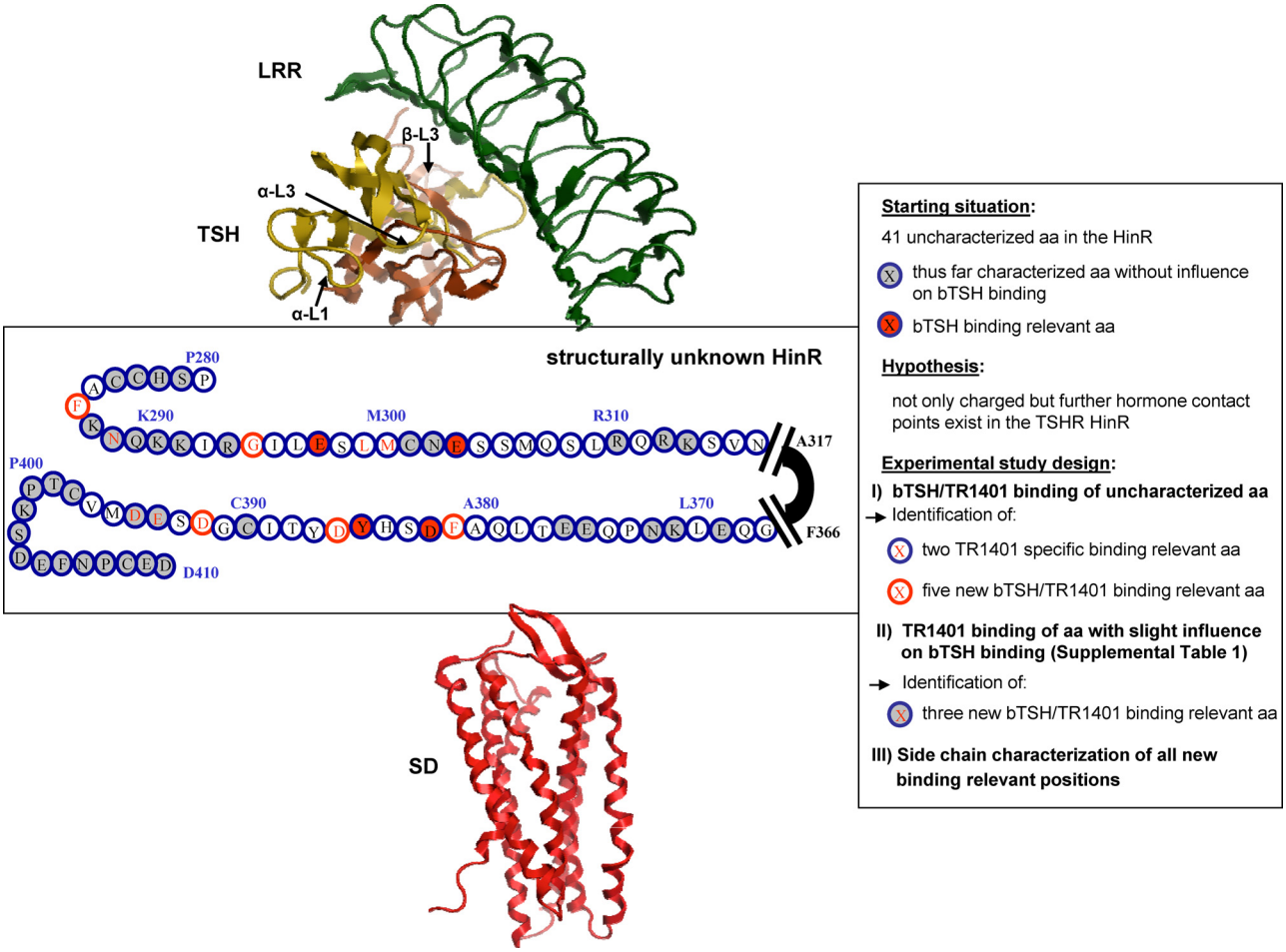

FIG. 1. Illustration of the TSHR composed of the LRR and serpentine domain (SD) structure, which is linked by the structural unknown hinge region investigated in this study. The comparative model of the LRR (depicted in *green*) is connected with the hTSH molecule represented in *yellow* (α-subunit) and *orange* (β-subunit). The surface-exposed loops (α-L1, α-L3, and β-L3), which have been shown to contribute to bTSH binding to the receptor are shown by *arrows*. As SD the crystal structure of the homologous CXCR 4 receptor (Protein Data Bank ID number: 3ODU) is shown in *red*. Based on the unknown exact junction between the LRR and the hinge region, there are different descriptions of its length (reviewed in Ref. 1). Assuming an extended LRR structure C-terminally from position L260, the hinge region starts at P280 in the present scheme. This structurally unknown region is shown by *circles* with the respective amino acid abbreviation except the cleavable 50-amino acid insertion, the so-called C-peptide from position A317–F366 (1). The experimental design of this study investigating the influence of single positions of the hinge region on hormone binding is shown in the *right box*.

tibody also provides only structural information for the particular LRR portion and not for the HinR (10).

Based on the identification of the first TSH binding sites in the HinR, it became apparent that multiple positions in this particular structure remained to be characterized. Moreover, it is very likely that beside the interaction of specific α-L1 residues of bTSH with negative charges of the HinR (8) further contact points of neighboring α-L1 or binding relevant α-L3 and β-L3 residues (11, 12), which obviously do not interact with the LRR (see Fig. 1) are located in the HinR. The goal of this study was to clarify whether more than the initially identified three contact points for receptor activation by TSH exist. Therefore, 41 so far uncharacterized residues located outside the C-peptide between P280 and D410 of the HinR were systematically analyzed. The impact on TSH binding of these residues was investigated by comparison of cell surface expression and bTSH binding. Whereas hydrophilic positions were substituted to alanine, selected hydrophobic positions were substituted to another hydrophobic residue of equal size for only slight side chain alterations due to the usually strong influence of hydrophobic residues on receptor conformation and structure stabilization.

We identified further 10 positions of the HinR, whose substitutions resulted in a strong decrease in bTSH binding compared with the respective expression value. bTSH has not only a higher affinity to the human (h) TSHR compared with hTSH but also superagonistic activity (13–18). Due to the low-affinity interaction of hTSH with its receptor it is not possible to use it in radioligand binding studies. To compare bTSH and hTSH binding, we therefore used the hTSH analog TR1401 (17), which differs with respect to its sequence from hTSH by only four additional positive charges in the α-L1. Our data show that

in addition to the previously identified amino acids of the LRR (4, 5) as well as the three negatively charged positions (7, 8) and the sulfation site Y385 (6), further 10 residues of this region seem to be crucial for bTSH and TR1401 binding.

Materials and Methods

Materials

Recombinant hTSH was obtained from Dr. A. F. Parlow (National Hormone and Peptide Program, Torrance, CA). For binding analysis, ^{125}I-bTSH was obtained from BRAHMS GmbH (Henningsdorf, Germany; 50 μCi/μg) and cold bTSH from Sigma Chemical Co. (St. Louis, MO). The human TSH analog TR1401, characterized by four substitutions (Q13K+E14K+P16K+Q20K; numbering is related to hTSH without signal peptide) in the α-subunit (17), was provided by Trophogen Inc. (Rockville, MD). TR1401 was produced and purified as previously described (8). This human TSH analog was ^{125}I labeled (specific activity: 50 μCi/μg) by PerkinElmer (Billerica, MA).

Site-directed mutagenesis

Mutations were introduced into the hTSHR via site-directed mutagenesis as previously described (8), whereas the human TSHR-pcDNA 3.1 hygro (−) was used as template.

Cell culture and transfection

COS-7 cells were transfected with the GeneJammer transfection reagent (Stratagene, Amsterdam, The Netherlands) as previously described (8), whereas a transfection efficiency of 50–60% of viable cells could be achieved for each experiment. Transfection of the wild-type (wt) hTSHR and the pcDNA3.1 vector alone was performed in each assay as control. Each binding or cAMP experiment was done simultaneously with a fluorescence-activated cell sorting (FACS) control from the same transfection.

FACS analysis

For determination of cell surface expression and transfection efficiency, FACS analysis was done as previously described (7) using the mouse antihuman TSHR monoclonal antibody 2C11 (MAK1281, Linaris, Wertheim, Germany) as primary antibody and the Alexa Fluor 488-conjugated goat antimouse IgG (Invitrogen, Eugene, OR). Receptor expression was determined by the mean fluorescence intensity using the LSR II (Becton Dickinson, San Jose, CA). The wt TSHR was set at 100% and mutant receptor expression was calculated according to this setting. The percentage of signal positive cells corresponds to transfection efficiency.

Radioligand binding assay

Competitive binding studies were performed as previously described (7, 19). The empty pcDNA3.1 vector was used as control. Maximal TSH binding capacity was calculated by nonlinear regression of competition binding curves using GraphPad Prism 4.0 (GraphPad Software, Inc., La Jolla, CA), assuming a one-site binding model (20). Maximal TSH binding of wt TSHR was set at 100% and the maximal binding capacity of all mutants was calculated according to this setting.

cAMP accumulation assay

cAMP accumulation was determined as previously described (8) using the cAMP AlphaScreen assay (PerkinElmer Life Sciences, Zaventem, Belgium) according to the manufacturer's instructions. The medium was supplemented with 100 mU/ml bTSH (Sigma) or 10 mU/ml hTSH (National Institutes of Health, National Institute of Diabetes and Digestive and Kidney Diseases, Bethesda, MD) or hTSH analog TR1401 (Trophogen) for TSHR stimulation.

Linear regression analysis (LRA) of constitutive activity as a function of TSHR expression

The characterization of the mutant's basal cAMP activity as a function of TSHR expression was done by an LRA determined by FACS as previously described (21).

Statistics

Statistical analysis was carried out by *t* test using GraphPad Prism 4.0 for Windows ($P < 0.001$, extremely significant; $P = 0.001–0.01$ very significant; $P = 0.01–0.05$, significant; $P > 0.05$, not significant).

Multiple sequence alignment

The conservation of amino acids within the TSHR HinR was evaluated by a multiple sequence alignment. Homologs were selected by searching the nonredundant protein sequences database using blastp (22) with the protein sequence of the hTSHR (gi 62298994). For further investigation, 16 Blast hits were selected by phylogenetic diversity. Full-receptor sequences were aligned with ClustalW2 (23) and formatted with Jalview (24). For evaluation of the conservation within the different human glycoprotein hormone receptor (GPHR), the alignment of the three receptors from the SSFA database (25) was used.

Structural modeling

The comparative model of the LRR connected with the hTSH was created using the Molecular Operating Environment software (MOE 2009.10; Chemical Computing Group, Inc., Montréal, Québec, Canada) with the crystal structure of FSH in complex with the LRR of the FSH receptor (FSHR) (9) as template. The crystal structure of the TSHR LRR (10) was used as environment during the generation of the homology model.

Results

This study was performed to identify further hTSHR positions of the HinR (1), which participate in hormone binding and subsequently to analyze the amino acid characteristics that are necessary to establish the hormone-HinR interaction (Fig. 1). The comparison between receptor expression and maximal bTSH binding (Bmax) of HinR mutants is compiled in Table 1.

TABLE 1. Comparison of TSHR cell surface expression measured by FACS analysis and maximal bTSH binding of TSHR hinge region mutants

hTSHR mutations of the hinge region	FACS analysis (% of wt TSHR)	Maximal bTSH binding (% of wt TSHR)
pcDNA	1.8 ± 0.1	—
TSHR wt	100	100
P280A	89.7 ± 2.0[a]	107.6 ± 1.0[a]
A285V	87.9 ± 4.4[b]	102.4 ± 1.4
F286A[c]	85.0 ± 4.8[b]	66.3 ± 2.2[a]
I292V	93.2 ± 3.0[b]	104.2 ± 3.5
G294A[c]	83.3 ± 5.8[b]	46.4 ± 1.3[a]
I295V	94.3 ± 3.0	99.2 ± 4.0
L296V	95.9 ± 2.7	103.7 ± 1.9
S298A	94.3 ± 1.9[d]	85.5 ± 2.5[a]
L299V	93.2 ± 2.6[b]	98.8 ± 3.5
M300V	89.7 ± 3.4[d]	85.8 ± 3.2[d]
S304A	67.5 ± 0.9[a]	85.5 ± 2.8[a]
S305A	104.8 ± 3.1	93.7 ± 1.6[a]
M306A	97.2 ± 2.6	105.3 ± 3.8
Q307A	91.4 ± 4.8	102.0 ± 1.3
S308A	77.6 ± 4.0[a]	102.7 ± 1.7
L309V	99.3 ± 1.4	99.1 ± 6.2
Q311A	91.3 ± 1.6[a]	90.7 ± 0.9[a]
S314A	93.2 ± 3.0[b]	86.7 ± 4.5[d]
V315A	91.8 ± 7.9	112.0 ± 1.4[d]
N316A	86.5 ± 2.6[a]	95.8 ± 1.4[b]
C-peptide (A317-F366)		
G367A	59.2 ± 2.6[a]	99.3 ± 3.8
Q368A	72.2 ± 5.8[a]	93.9 ± 2.5
L370V	97.5 ± 1.4	99.8 ± 2.2
P373A	94.8 ± 5.8	105.1 ± 4.8
Q374A	79.5 ± 3.1[a]	75.2 ± 3.0[a]
T377A	94.3 ± 2.1[b]	91.6 ± 5.1
L378V	94.9 ± 2.6	99.5 ± 3.6
Q379A	97.1 ± 3.1	82.6 ± 2.5[a]
A380V	87.0 ± 6.5	84.0 ± 1.8[a]
F381A[c]	90.3 ± 2.8[a]	60.6 ± 1.3[a]
S383A	95.8 ± 3.5	114.5 ± 2.0[a]
H384A	95.9 ± 6.8	92.6 ± 1.3[a]
D386A[c]	98.8 ± 3.1	76.8 ± 3.4[a]
Y387A	88.6 ± 3.4[d]	90.2 ± 1.5[a]
T388A	99.0 ± 5.0	103.4 ± 1.7
I389V	94.7 ± 1.1[a]	90.1 ± 2.0[a]
G391A	64.6 ± 2.6[a]	74.2 ± 1.1[a]
D392A[c]	92.3 ± 8.5	76.7 ± 2.5[a]
S393A	96.0 ± 4.8	87.0 ± 2.7[a]
M396V	101.0 ± 2.7	104.3 ± 2.1
V397I	93.8 ± 1.7[d]	89.9 ± 4.0[b]

Twenty mutants of the N-terminal and 21 mutants of the C-terminal part of the hTSHR hinge region were analyzed regarding differences between FACS and maximal bTSH binding. Hydrophobic residues were individually exchanged mainly by another hydrophobic amino acid (A, I, L, M→V or F, V→A, I) due to the strong influence of hydrophobic residues on the receptor conformation and stabilization of the structure. All other amino acids were substituted by an alanine. The cleavable C-peptide region (A317-F366) is represented by extra space. Data are given as mean ± SEM of at least three independent experiments, each carried out in duplicate. The wt TSHR and empty pcDNA vector were used as controls. $P > 0.05$, not significant.

[a] $P < 0.001$, extremely significant.

[b] $P = 0.01–0.05$, significant.

[c] Mutants with a significantly reduced (>15%) bTSH binding compared with the respective FACS value.

[d] $P = 0.001–0.01$, very significant.

Novel TSH binding sites of the HinR

All mutants showed an expression comparable with the wt in the range of 72–105% except S304A, G367A, and G391A with a receptor expression in the range of 59–68%. Most mutants revealed a Bmax of bTSH similar to the respective FACS results, whereas the expression of mutants S308A, G367A, and Q368A was significantly reduced (>21%) compared with the binding result. In contrast, the five mutants, F286A, G294A, D386A, F381A, and D392A, revealed a significant decrease of the bTSH Bmax value by 15–37% compared with wt and to the respective FACS value. Four of the five mutants showed a stronger decrease of hTSH analog TR1401 compared with bTSH binding, whereas D386A led to a reduced TR1401 binding comparable with bTSH. Moreover, mutants L299V and M300V showed an expression and bTSH binding pattern comparable with the wt, whereas TR1401 binding was reduced to 68 and 61%, respectively (Supplemental Table 1, published on The Endocrine Society's Journals Online web site at http://endo.endojournals.org).

A summary of TSH binding data for all positions of the HinR (Supplemental Table 1) shows that alanine mutation of the known TSH binding relevant sulfation site Y385 led to a minimal binding capacity of TR1401 with only 15% of wt. Moreover, with N288, E394, and D395, the HinR summary (Supplemental Table 1) provides three previously characterized HinR positions with slight influence on hormone binding. Expression of N288A was previously reported to be 82% of wt (21). The new hormone binding data revealed a reduced bTSH (60% of wt) and TR1401 (47% of wt) binding capability. Furthermore, alanine substitution at E394 and D395 showed a slightly decreased bTSH binding and in case of E394A also in TR1401 binding compared with the wt and to the respective FACS value.

Side-chain characterization of binding sites

To identify potential amino acid characteristics necessary for maintaining the hormone-HinR interaction at the binding positions, side-chain substitutions with different amino acid properties were performed and functionally characterized (Table 2). No constitutive activity was detected for all analyzed mutations. Due to the known relatively low-affinity interaction of hTSH with the hTSHR (26), which leads to very low detectable ^{125}I-hTSH binding (27, 28), we are limited to signaling studies with hTSH.

Position F286

The hydrophobic, aromatic F286 was substituted to tryptophan with similar amino acid characteristics as well as to the hydrophobic and branched isoleucine. Changing

TABLE 2. Functional characterization of side-chain variations of hormone binding sites within the hTSHR hinge region

hTSHR mutations of the hinge region	FACS analysis (% of wt TSHR)	Maximal bTSH binding (% of wt TSHR)	Maximal TR1401 binding (% of wt TSHR)	cAMP accumulation (% of wt TSHR)			
				Basal	Hormone stimulated		
					bTSH	TR1401	hTSH
pcDNA	1.8 ± 0.1	—	—	51.0 ± 9.2	2.5 ± 0.4	4.3 ± 0.6	5.3 ± 0.7
TSHR wt	100	100	100	100	100	100	100
F286							
A	85.0 ± 4.8[a]	*66.3 ± 2.2*[b]	**31.2 ± 1.2**[b]	101.2 ± 11.1	96.1 ± 6.5	83.5 ± 5.6	**55.3 ± 7.3**[b]
I	106.1 ± 4.6	**28.9 ± 1.8**[b]	**18.9 ± 0.8**[b]	76.6 ± 6.4[c]	**63.4 ± 1.5**[b]	91.6 ± 5.9	**54.9 ± 5.6**[b]
W	86.8 ± 3.7[c]	95.1 ± 3.2	78.0 ± 2.6[b]	79.8 ± 4.7[b]	87.7 ± 7.0	90.2 ± 3.0[c]	105.7 ± 5.7
N288							
A	82 (21)	*60.3 ± 1.2*[b]	**46.9 ± 1.5**[b]	110 (21)	*66% (21)*	*60.4 ± 5.5*[b]	**47.0 ± 5.4**[b]
L	100.9 ± 3.1	*67.6 ± 3.3*[b]	**46.1 ± 0.9**[b]	84.3 ± 10.1	*70.3 ± 5.8*[b]	**52.4 ± 4.2**[b]	**42.3 ± 1.9**[b]
Q	107.4 ± 4.0	*80.0 ± 3.0*[b]	*69.4 ± 2.6*[b]	109.1 ± 11.3	*65.3 ± 3.7*[b]	*63.3 ± 6.3*[b]	**52.8 ± 4.5**[b]
S	93.2 ± 3.1[a]	100.0 ± 3.8	81.2 ± 4.5[b]	122.1 ± 12.8	*76.0 ± 3.6*[b]	*60.2 ± 1.8*[b]	*68.2 ± 3.9*[b]
G294							
A	83.3 ± 5.8[a]	**46.4 ± 1.3*[b]***	**16.0 ± 1.0**[b]	99.0 ± 19.6	97.0 ± 9.0	98.5 ± 4.5	81.6 ± 8.3
I	104.5 ± 4.6	**23.3 ± 1.8**[b]	**18.9 ± 1.2**[b]	91.8 ± 12.4	**47.6 ± 3.2**[b]	*78.7 ± 4.7*[c]	**54.5 ± 4.2**[b]
S	96.5 ± 2.4	98.6 ± 1.5	*75.3 ± 2.6*[b]	104.6 ± 15.5	*68.1 ± 4.7*[b]	88.5 ± 1.6[b]	86.6 ± 3.2[b]
L299							
A	97.7 ± 6.2	92.3 ± 3.9[b]	*69.1 ± 2.1*[b]	115.8 ± 12.6	*73.0 ± 4.6*[b]	95.3 ± 5.3	*65.4 ± 7.0*[b]
D	72.6 ± 4.6[b]	70.2 ± 5.5[b]	*46.2 ± 1.4*[b]	90.0 ± 11.9	*65.2 ± 3.9*[b]	103.0 ± 6.8	*68.3 ± 5.5*[b]
I	86.6 ± 4.9[a]	104.6 ± 2.0[b]	99.8 ± 5.9	100.3 ± 16.9	*77.2 ± 4.8*[b]	99.8 ± 5.1	106.7 ± 5.9
V	93.2 ± 2.6[a]	*98.8 ± 3.5*	*67.9 ± 4.4*[b]	85.2 ± 19.2	*74.5 ± 6.7*[c]	*78.8 ± 4.6*[b]	83.7 ± 5.1[c]
M300							
A	78.7 ± 6.2[c]	*60.2 ± 2.4*[b]	66.3 ± 3.0[b]	133.8 ± 11.6[a]	93.3 ± 7.1	**53.1 ± 5.2**[b]	*66.5 ± 3.3*[b]
D	61.0 ± 4.3[b]	*36.5 ± 0.8*[b]	*40.7 ± 2.5*[b]	106.7 ± 10.2	*71.1 ± 5.5*[b]	*71.4 ± 5.8*[b]	*67.6 ± 5.9*[b]
L	87.3 ± 4.5[a]	73.3 ± 1.9[b]	77.8 ± 2.4[b]	90.2 ± 21.1	83.9 ± 6.6[a]	84.8 ± 3.7[c]	90.7 ± 6.1
V	89.7 ± 3.4[c]	*85.8 ± 3.2*[c]	*60.9 ± 6.4*[b]	88.0 ± 15.5	*79.5 ± 5.5*[c]	*78.2 ± 4.2*[a]	92.4 ± 4.9
F381							
A	90.3 ± 2.8[b]	*60.6 ± 1.3*[b]	**48.8 ± 1.1**[b]	149.0 ± 10.3[b]	*60.8 ± 3.7*[b]	86.0 ± 3.9[c]	80.7 ± 4.1[b]
D	61.3 ± 2.7[b]	62.4 ± 1.2[b]	66.5 ± 3.4[b]	157.4 ± 17.8[c]	*66.1 ± 5.2*[b]	*76.3 ± 4.5*[b]	*70.0 ± 6.3*[b]
I	94.9 ± 1.2[b]	**45.4 ± 1.3**[b]	**52.6 ± 2.7**[b]	136.5 ± 9.6[c]	86.3 ± 9.0	80.0 ± 4.9[c]	85.5 ± 5.3[a]
K	88.7 ± 1.4[b]	**18.2 ± 1.0**[b]	**20.0 ± 1.1**[b]	144.3 ± 11.7[c]	*64.8 ± 7.6*[b]	*70.8 ± 4.6*[b]	*60.7 ± 4.2*[b]
Q	91.2 ± 1.6[b]	**45.1 ± 2.7**[b]	**48.6 ± 3.3**[b]	155.4 ± 10.9[b]	80.3 ± 7.8[a]	*71.5 ± 6.0*[b]	*64.7 ± 5.9*[b]
V	94.5 ± 2.1[a]	**37.7 ± 1.3**[b]	**49.0 ± 3.2**[b]	140.8 ± 15.8[a]	*71.2 ± 7.6*[c]	81.2 ± 5.1[c]	94.5 ± 4.8
Y	91.2 ± 3.4[a]	85.3 ± 2.2[b]	98.6 ± 3.4	164.1 ± 11.3[b]	101.7 ± 9.7	86.3 ± 3.2[c]	98.7 ± 2.8
D386							
A	98.8 ± 3.1	*76.8 ± 3.4*[b]	*75.2 ± 1.9*[b]	94.2 ± 7.2	*77.0 ± 4.8*[b]	**52.8 ± 6.1**[b]	**51.8 ± 4.8**[b]
E	101.3 ± 3.4	104.2 ± 1.9[a]	118.0 ± 3.3[b]	112.3 ± 10.1	95.9 ± 6.1	*73.7 ± 7.3*[c]	*67.5 ± 7.1*[c]
K	89.0 ± 3.4[a]	**23.2 ± 0.4**[b]	**19.7 ± 2.4*[b]***	98.3 ± 11.3	**36.2 ± 4.5**[b]	*76.3 ± 4.8*[a]	**33.1 ± 4.2**[b]
D392							
A	92.3 ± 8.5	*76.7 ± 2.5*[b]	*60.6 ± 2.1*[b]	110.8 ± 5.0	84.8 ± 8.0	86.1 ± 6.2	*59.5 ± 7.0*[b]
E	96.1 ± 2.3	93.5 ± 2.1[a]	103.4 ± 5.1	93.4 ± 7.1	88.8 ± 4.3[a]	106.5 ± 3.8	106.6 ± 5.1
K	94.8 ± 3.2	**48.0 ± 2.1**[b]	**38.9 ± 2.1**[b]	66.1 ± 9.9[c]	**43.2 ± 2.1**[b]	82.0 ± 4.9[c]	**51.4 ± 5.2**[b]
E394							
A	93 (7)	*71* (7)	79.5 ± 3.6[b]	127.3 ± 23.1	*59.3 ± 2.8*[b]	*54.9 ± 3.0*[b]	*64.8 ± 8.2*[c]
D	97.1 ± 3.4	106.3 ± 4.0	105.8 ± 1.5[c]	137.3 ± 19.5	92.7 ± 4.7	84.8 ± 7.7	*75.3 ± 4.1*[b]
K	91.2 ± 2.5[c]	**26.2 ± 0.5**[b]	**51.9 ± 1.4**[b]	87.1 ± 11.6	*57.3 ± 3.6*[b]	80.9 ± 5.5[c]	83.7 ± 7.8
D395							
A	85 (7)	*70* (7)	87.1 ± 1.9[b]	100.8 ± 5.4	**52.5 ± 5.9**[b]	**46.2 ± 3.2**[b]	**55.8 ± 4.3**[b]
E	103.9 ± 4.5	99.8 ± 1.9	93.5 ± 2.1[c]	129.4 ± 19.6	98.4 ± 2.9	106.1 ± 6.1	105.9 ± 5.1
K	76.8 ± 4.0[b]	77.3 ± 2.1[b]	*61.3 ± 1.9*[b]	99.3 ± 7.2	*67.4 ± 7.1*[b]	*67.9 ± 7.4*[c]	*63.0 ± 4.5*[b]

Cell surface expression measured by FACS analysis, bTSH and TR1401 analog binding, and basal and TSH-stimulated cAMP response are listed for the side-chain substitutions of all newly identified hinge positions with an effect on hormone binding. For a complete overview, some data of Table 1 and previously published findings (marked with the specific reference) were included. Data are given as mean ± SEM of at least three independent experiments, each carried out in duplicate. The wt TSHR and empty pcDNA vector were used as controls. Reduced binding and maximal cAMP values are shown in *italics* and *bold* (binding: 15–35% binding reduction, *italics*; greater than 35% reduction, *bold*; signaling: maximal cAMP value with 60–80% of wt, *italics*; less than 60% of wt, *bold*). $P > 0.05$, not significant.

[a] $P = 0.01$–0.05, significant.

[b] $P < 0.001$, extremely significant.

[c] $P = 0.001$–0.01, very significant.

phenylalanine to tryptophan led to a Bmax of bTSH similar to the wt and the respective FACS value, whereas introduction of an isoleucine results in a decreased bTSH binding to 29% of the wt (Table 2). Moreover, F286I showed a strong decrease of TR1401 binding. In contrast, F286W resulted in TR1401 binding similar to the respective FACS result analogous to bTSH binding. Furthermore, hTSH, bTSH, and TR1401 stimulation of F286W led to a cAMP response similar to the wt. However, despite the reduced Bmax from 66 to 19% of wt, F286A and F286I revealed maximal cAMP stimulation in the range of 63–96% after stimulation with bTSH or TR1401. In con-

trast, using hTSH, both mutations showed a maximal cAMP signaling of only 55% of wt.

Position N288

In addition to alanine, hydrophilic asparagine at position 288 was exchanged to hydrophilic glutamine, smaller serine, and hydrophobic leucine. All three single mutants revealed an expression similar to the wt. Similar to the alanine mutant, N288L reduced bTSH binding to 68% and TR1401 binding to 46% of wt. Substitution to serine led to a bTSH and TR1401 binding similar to the wt or only to a slight decrease (Table 2). However, bTSH and TR1401 binding of N288Q was slightly decreased compared with the respective FACS value. All mutants at position N288 led to a reduced maximal cAMP signal in the range of 42–76% of wt.

Position G294

Side-chain characterization for G294 was carried out by changing the hydrophilic and small glycine to the small and hydrophilic serine and to the branched hydrophobic isoleucine. G294S showed a bTSH binding similar to that of the wt and to the respective FACS result, whereas G294I revealed a decrease in bTSH binding with only 23% (Table 2). Furthermore, G294I led to a TR1401 binding of only 19% of the wt similar to G294A with 16% binding capacity. However, G294S showed with 75% a slightly reduced maximal TR1401 binding compared with the respective FACS value. In addition to the strong reduction of bTSH and TR1401 binding by mutant G294A, both TSH variants led to a maximal cAMP signaling similar to the wt. Moreover, stimulation with hTSH resulted in a slightly decreased cAMP production of mutant G294A. G294I showed a reduced cAMP accumulation after stimulation with all three investigated TSH variants and G294S only after addition of bTSH.

Positions L299 and M300

Side-chain characterization was done by substitution of the hydrophobic leucine or isoleucine and by the small hydrophobic alanine. Based on the close sequence proximity of the negatively charged TSH binding sites E297 and E303, the charge influence of positions L299 and M300 on hormone binding was analyzed by introduction of the negatively charged aspartic acid. The expression of L299A and L299I was 98 and 87% of the wt, respectively (Table 2). The lowest expression rate of the three mutations at residue L299 was 73% for L299D. Moreover, all four mutants at position L299 showed a Bmax of bTSH comparable with the respective FACS value. However, maximal TR1401 binding was reduced to 68% for L299A and L299V and to 46% for L299D, whereas L299I showed a Bmax of TR1401 at the expression level. The four mutants at position M300 revealed an expression in the range of 61–90% of wt and a decreased bTSH binding for M300A, M300D, and M300L, with M300D being the most prominent with only 37%. However, M300V showed a bTSH binding comparable with the respective FACS value. Moreover, maximal TR1401 binding was similar to bTSH binding for M300A, M300D, and M300L, in contrast to M300V, which showed with 61% a decrease compared with the respective expression and bTSH binding result. Except M300A with a reduction of the cAMP level to 53% of wt after stimulation with TR1401, all mutants at L299 and M300 showed no or only a slight decrease after stimulation with all three TSH variants. The basal cAMP accumulation was slightly enhanced for M300A, but LRA revealed no constitutive activity (data not shown).

Position F381

The aromatic residue F381 was exchanged to the aromatic tyrosine and to the hydrophobic valine and isoleucine as well as to the hydrophilic glutamine. Apart from F381Y with a bTSH binding capability similar to the respective FACS value, all three substitutions showed a reduced Bmax of bTSH (in the range of 18–45% of the wt). Due to the previously identified charge-charge interaction of bTSH with the direct neighbor D382 (7, 8), we introduced a positive and also a negative charge at position F381 to analyze the charge influence on hormone binding. F381D showed a Bmax comparable with the respective FACS value, whereas F381K led to a reduced bTSH binding to 18% of the wt in contrast to the FACS result with 89% (Table 2). Moreover, TR1401 binding showed similar results like bTSH in the range of 18% (F381K) to 99% (F381Y) compared with the wt (Table 2). Despite the strongly reduced bTSH and TR1401 binding capacity of all substitutions at F381, except F381Y, the stimulated cAMP responses after stimulation with bTSH, TR1401 and hTSH were not or only slightly decreased. F381Y showed no alteration in maximal cAMP results for all three TSH variants. Although all seven substitutions at F381 led to slightly increased basal cAMP values, LRA showed no constitutive activity (data not shown).

Position D386

The negatively charged aspartic acid was substituted by the charge-keeping glutamic acid and the positively charged lysine. Substitution of aspartic acid to lysine with the opposite charge characteristic led to a decrease in bTSH and also TR1401 binding, with about 20% of maximal hormone binding, respectively, compared with the wt. In contrast, maintaining the negative charge by glutamic acid results in a Bmax of bTSH similar to the wt as

well as to a slight enhanced TR1401 binding with 118% of wt (Table 2). Except for D386E stimulation of all other substitutions at this position with bTSH, hTSH and TR1401 showed a reduced cAMP signal in a range between 33 and 77% when compared with the wt. No constitutive activity could be detected for all substitutions at this position.

Position D392

Side-chain characterization for the negatively charged position D392 was performed using the charge-keeping glutamic acid as well as lysine with the opposite charge characteristic. Maximal bTSH and TR1401 binding for D392E was similar to that of the wt, whereas D392K led to a decrease in bTSH as well as TR1401 binding with only 48 and 39% of hormone binding, respectively, compared with the wt (Table 2). TR1401 binding at D392A was reduced to 61%. All mutants at position D392 showed no constitutive activity. However, D392K revealed a significantly decreased stimulation using bTSH and hTSH but not after TR1401 addition.

Positions E394 and D395

The negatively charged residue of both positions was substituted to an amino acid of the opposite charge characteristic and also to a charge-keeping residue. In addition to D395K, with an expression of 77%, all other three mutants were expressed similar to the wt (Table 2). However, Bmax of bTSH was reduced to 26% for E394K but not for D395K, with a bTSH binding similar to the respective expression. In contrast, TR1401 binding was reduced for both lysine mutations to 52% (E394K) or 61% (D395K) of wt. However, D395E and E394D showed a bTSH and TR1401 binding similar to the FACS results. Moreover, these mutants led to hTSH-, bTSH-, and TR1401-mediated cAMP stimulation similar to the wt or only to a slight decrease. E394A, D395A, and D395K resulted in a reduced cAMP accumulation in the range of 46–68% of wt.

Discussion

The importance of the HinR for hormone binding, signal transduction, and receptor activation has been indicated in several studies (reviewed in Ref. 1). However, the hormone-TSHR interaction mechanisms are only incompletely understood. Recently it was suggested that the binding relevant HinR is possibly altered in its conformation by the adjacent serpentine domain, which therefore also influences indirectly ligand binding (29). Thus, the knowledge about the contribution of the HinR to hormone binding is important for further elucidation of the precise molecular hormone-receptor interactions.

The present study revealed that further positions of the TSHR HinR, namely F286, G294, L299, M300, F381, D386, and D392, are also involved in TSH binding. Moreover, characterization of Bmax for previously described mutations of the HinR (Supplemental Table 1) and subsequent side-chain characterization identified further positions: N288, E394, and D395 with influence on hormone binding.

In this study, we focused on the significant decrease in Bmax of TSHR mutants in comparison with their expression levels without taking possible alterations of IC_{50} or dissociation constant (Kd) values into account. Kd or IC_{50} results of the investigated mutants of the hormone binding sites are difficult to interpret due to the strong differences in the maximal binding capacity. For an appropriate evaluation and comparison of Kd values, it would be necessary to express all receptor constructs at the same Bmax level, for which numerous titration experiments would be necessary. However, such information and the possibility that the Kon to Koff ratio of TSH binding could be altered by the mutants do not affect our main finding that further HinR residues affect TSH-TSHR interaction as this interpretation is primarily based on the decrease of the maximal TSH binding capacity of these mutants.

Five of the newly identified TSH binding sites are located N and the other five C terminally of the C-peptide (Table 1 and Supplemental Table 1). With D386, D392, E394, and D395, four further negative charges of the HinR influence hormone binding. Due to the new finding that also F286 and F381 influence bTSH binding, the question arises of whether besides identified charge-charge interactions (8), there could be further interrelations like hydrophobic interactions between the HinR and the hormone. To address the question of which potential amino acid characteristics of the binding sites are necessary, functional characterization of side-chain substitutions was performed.

Hormone binding cluster F381-D386

Costagliola *et al.* (6) showed that sulfation on Y385 within the YDY-motif (Fig. 2) is necessary for high affinity bTSH binding at the hTSHR. The present results demonstrate a strong influence of Y385 also on TR1401 binding (Supplemental Table 1). In addition to this conserved YD/EY-motif of GPHR (Fig. 2) (6, 30), the neighboring TSHR position D382 (7) as well as the homologous D330 of the LH/choriogonadotropin (CG) receptor (31) were identified as key residues of binding or receptor activation. The TSHR region K371-H384 was identified as essential for TSH binding (32). Hamidi *et al.* (33) showed that a similar

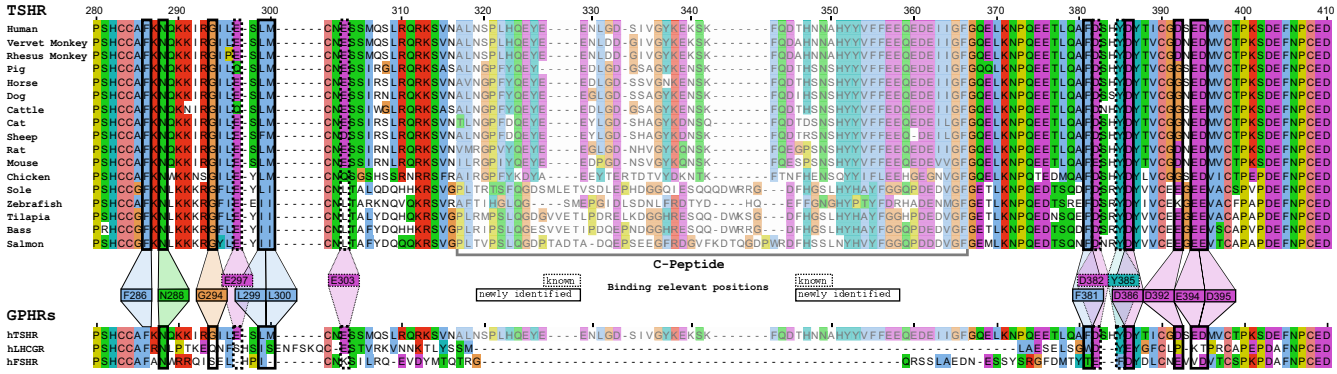

FIG. 2. Hinge region amino acid sequence alignment of different TSHR species and the homologous hFSHR and hLH/CGR. For the present alignment, we assumed that based on the hypothesis of an extended LRR structure from position L260 to Y279 (1), amino acids P280–D410 including the C-peptide from position A317 to F366 constitutes the TSHR hinge region, which was investigated in the present study. Previously published and newly identified binding sites of the hinge region, which are located N- and C-terminally of the C-peptide are highlighted by *boxes*.

region, namely T377-H384, contributes to ligand binding and cAMP signal transduction, whereas deletions of region Q307-K371 and E303-F366 were tolerated without alterations in bTSH binding and signaling. A summary of functional characterization of HinR residues (Supplemental Table 1) did not show TSH binding sites within these two regions, with one exception. Thus, position E303 located on the edge of region E303-F366 has been shown to participate in bTSH and TR1401 binding. However, it does not have such a strong effect as the previously identified residues E297 and D382 (7, 8). With the present study, we identified neighboring positions F381 and D386 as also important for bTSH and TR1401 binding. Thus, all positions located in sequence proximity: T377-H384 (33) containing D382 (7) and F381 as well as Y385 (6) and D386 are relevant for TSH binding. This bTSH/TR1401-binding domain extends from the F381 to D386, whereas the adjacent A380 and Y387 as well as S383 and H384 within this binding cluster are obviously not involved in bTSH and TR1401 binding.

Szkudlinski *et al.* (34) reviewed that charge-charge interactions are of major importance in TSH-TSHR interaction. From the evolutionary point of view, it is well known that additional positive charges at specific residues of TSH and CG improve receptor affinity (17, 35). For TSHR position D382, a charge-charge interaction with positive α-L1 charges of bTSH and TR1401 is assumed (Fig. 1A in Ref. 8). Based on the sequence proximity to D382, we would expect an interaction scenario between the other residues of the cluster F381-D386 and α-L1 positions of bTSH and TR1401, respectively. However, possible specific interaction combinations between bTSH residues and the hTSHR positions have to be studied more extensively by further experiments. Moreover, in addition to the direct involvement of positions within F381-D386 in TSH binding, it is also conceivable that some residues affect the overall structure of this region. As a direct neighbor of Y385, it could also be possible that mutations at D386 indirectly influence TSH binding via interference with the sulfation process. However, side-chain characterization for D386 revealed that this position rather seems to interact via charge-charge interplay with bTSH. Thus, introduction of a positive charge at D386 led to a strong decrease in TSH binding indicating electrostatic repulsion of positive hormone charges.

In addition to the great variation of the GPHR HinR in size and amino acid sequence, the negative charge at position D386 is conserved within several TSHR species and also at homologous FSHR and LH/CG receptor (LH/CGR) positions (Fig. 2), indicating a general or class-specific impact of this charge on glycoprotein hormone (GPH) binding. However, the question about hTSH binding remains open due to the known relatively low-affinity interaction of hTSH with the hTSHR (26), which leads to very low detectable ^{125}I-hTSH binding (27, 28). Thus, hTSH interaction with the hTSHR and the role of the identified bTSH binding sites and their differences to the superagonistic bTSH have to be elucidated by further methods like fluorescence resonance energy transfer investigations, which enable direct binding analysis of hTSH.

Furthermore, we cannot conclude from maximal TSH stimulated cAMP values on TSH binding capacity. For example, despite the impaired maximal TR1401 binding of D386K (20% of wt), this mutation led to a maximal cAMP stimulation of 76%. Such a mutant phenotype with a reduced TSH binding but a cAMP signaling similar to the wt has previously been shown for other substitutions like D382K (8), C462S, and C600S (36). TR1401 and bTSH both showed a strong reduction of Bmax on D386K, but bTSH led to a 2-fold stronger decrease of the maximal cAMP signaling compared with TR1401 (Table 2). This indicates differences in the coupling of ligand binding with

cAMP signal transduction between TR1401 and bTSH at position D386.

Side-chain characterization for F381 revealed that only the aromatic tyrosine maintains bTSH and TR1401 binding (Table 2). Therefore, we assumed either a stabilizing structural effect of F381 or a direct aromatic interaction with the hormone. Given that the direct neighbor D382 interacts with the positive α-L1 charges (K11 or K14, K13, K16, K20) of TR1401 and bTSH (8), it is very likely that F381 also interacts with residues of α-L1. Indeed, with the neighboring aromatic residues of bTSH (Y17, F18) and TR1401 (F17, F18) [Fig. 1 in the report of Mueller *et al.* (8)], there are potential interaction partners for F381 or tyrosine substitution. Such noncovalent aromatic interactions have been shown to participate in protein-ligand interactions (37), but they have to be verified by further studies in the case of HinR-TSH interaction. The strongest reduction of TSH binding was shown for the introduction of a positive charge at F381. This is most likely due to the release of the stabilizing effect or the aromatic interaction and in addition to disruption or electrostatic repulsion of adjacent charge-charge interactions, *e.g.* between D382 and positive α-L1 charges of bTSH and TR1401, respectively. Based on the alignment of several TSHR species (Fig. 2), which shows a complete conservation of phenylalanine at F381, the importance of this residue becomes apparent. In contrast, homologous positions at the hFSHR and hLH/CGR reveal no conservation of phenylalanine. However, with tryptophan in the hLH/CGR and a tyrosine as the N-terminal adjacent position in the hFSHR the aromatic characteristic is maintained at the homologous F381 position or its proximity (Fig. 2), suggesting a stabilizing effect or aromatic interactions also for the other two GPHRs. Despite the conserved YD/EY-motif and the conservation of the negative charge at D382, D386, and homologous GPHR positions, it still remains to be elucidated whether the homologous regions of the TSHR cluster F381-D386 are also important for hFSH-hFSHR and hLH/CG-hLH/CGR interaction.

D392, E394, D395: charge influence on hormone binding

Side-chain characterization at position D392 revealed that the negative charge is essential for maintaining bTSH and TR1401 binding. Thus, introduction of a positive charge at D392 obviously led to electrostatic repulsion of positive charges at the hormone. However, the negative charge is not completely conserved among selected TSHR species and exists in hFSHR but not in hLH/CGR (Fig. 2). Discrepancies between maximal cAMP signaling of D392K using TR1401 and bTSH despite a similar Bmax value (Table 2) indicate differences between bTSH and TR1401 in the transition from ligand binding to cAMP signal transduction for D392. The summary of expression and TSH binding data for all positions of the HinR (Supplemental Table 1) provides with E394 and D395 two further negatively charged HinR residues with influence on hormone binding. The negative charge of E394 and to a lesser extent of D395 is also important for bTSH and TR1401 binding. However, both negative charges are conserved within several TSHR species, whereas only the charge of D395 exists at the homologous position of the hFSHR (D343) but not of the hLH/CGR (Fig. 2). Future studies have to clarify which positive charge at bTSH does interact with D392 and whether the homologous D343 of the hFSHR is also involved in FSH binding.

Further N-terminally located hydrophobic and hydrophilic residues with impact on TSH binding

The present study reveals that in addition to E297 and E303 (7), F286, N288, G294, L299, and M300 participate in TSH binding. The maintaining of wt function if F286 is substituted to tryptophan demonstrated that the aromatic characteristic is necessary for bTSH and TR1401 binding. Position F286 not only influences bTSH and TR1401 binding but also hTSH signaling. In contrast to TR1401 and bTSH, stimulation of F286A and F286I with hTSH revealed a strong decrease of the maximal cAMP response. Such differences in maximal cAMP signaling of TSHR mutants between hTSH and bTSH stimulation raise the question of whether the data with the superagonistic bTSH at the hTSHR, which is in the majority of cases used for *in vitro* studies, are representative for the natural ligand hTSH.

The aromatic property of F286 is not only conserved within several TSHR species but also at homologous hFSHR and hLH/CGR positions (Fig. 2). Thus, it is very likely that the aromatic F286 and homologous FSHR and LH/CGR positions contribute to either a stabilizing structural effect or a direct noncovalent aromatic interaction with the hormone. This was also assumed for F381. A further evidence for the binding sensitivity of F286 and also for the neighboring N288 was demonstrated by Morris *et al.* (38), who identified the region F286-S305 as a specific hormone binding region. Asparagine 288 is conserved within several TSHR species and at homologous hFSHR and LH/CGR positions (Fig. 2). Side-chain substitutions at N288 revealed that maintaining TSH-HinR interaction depends most likely on the hydrophilic character (Table 2). This could also be shown for G294, in which glycine is conserved within several TSHR species (Fig. 2), and the hydrophilic property is conserved at the homologous positions of the hFSHR (S286) and LH/CGR (Q290).

The summary of expression and TSH binding data for all positions of the HinR (Supplemental Table 1) provided with L299 and M300 two hydrophobic HinR residues with influence on hormone binding, located between the known binding sites E297 and E303 (7). By side-chain substitutions, it was shown that in case of L299 substitution to isoleucine led to a binding property similar to the wt. Similar results were obtained for M300L. The hydrophobic property of both positions is conserved within several TSHR species (Fig. 2). However, in contrast to M300, the homologous positions of L299 at the FSHR and LH/CGR also display with isoleucine a hydrophobic residue. Additional negative charges at both positions do not support the charge-charge interplay between E297 and/or E303 with the positive charges of the hormone α-L1 (8) but rather interrupt TSH-HinR interaction. It remains to be elucidated whether besides the charge-charge interactions at E297 and E303 (8) there are also simultaneous hydrophobic interactions between the HinR and TSH.

Taken together, this is the first systematic mutational analysis of the TSHR HinR using two different TSH ligands. Our study provides evidence of the following: 1) besides the LRR, the sulfation site Y385 and the three known negatively charged residues further 10 positions of the HinR are involved in bTSH and hTSH analog TR1401 binding; 2) the newly identified multiple interaction sites are scattered along the HinR, whereas a cluster of binding sites seems to exist at region F381-D386; and 3) among the identified positions, four further charged residues could be detected, which participate in hormone binding via charge-charge interactions. Nevertheless, HinR-TSH interaction obviously does not exclusively exist as electrostatic interactions because hydrophobic and hydrophilic properties at HinR residues also are necessary to maintain hormone-receptor binding. Therefore, appropriate counterparts at the TSH also display potential targets for hormone modifications leading to alterations of receptor binding.

Most important in addition to previous evolutionary strategies focusing only on the hormone, these results will provide a complementary approach for a receptor-driven generation and optimization of orthosteric antagonists, inverse agonists, and also improved TSH analogs focusing on the binding and activation relevant HinR.

Thus, the results of the present receptor-based investigation of TSH-TSHR interactions and especially the provided specific characteristics of the HinR binding sites should lead to further studies, which will disclose the direct interaction partners at the hormone molecule. Such findings should also provide further insights into the molecular basis of GPH-GPHR interactions.

Acknowledgments

We thank Anja Moll and Saskia Fiedler for their excellent technical assistance. The authors acknowledge Dr. Bruce D. Weintraub, Dr. Valerie Fremont, Dr. Meng Zhang, and other colleagues at Trophogen that contributed to the development, production, purification, and characterization of TR1401.

Address all correspondence and requests for reprints to: Professor Dr. Med. Ralf Paschke, Division of Endocrinology and Nephrology, University of Leipzig, Liebigstraße 20, D-04103 Leipzig, Germany. E-mail: Ralf.Paschke@medizin.uni-leipzig.de.

This work was supported by the Medical Faculty, University of Leipzig Nachwuchsförderprogramm (NBL Formel.1-108) and grants from the Deutsche Forschungsgemeinschaft (DFG/Pa 423/15-1, 2 and DFG/Pa 423/14-1, 2 and DFG/Ja 1927/1-1).

Disclosure Summary: The authors have nothing to disclose.

References

1. **Mueller S, Jaeschke H, Günther R, Paschke R** 2010 The hinge region: an important receptor component for GPHR function. Trends Endocrinol Metab 21:111–122
2. **Chazenbalk GD, Tanaka K, Nagayama Y, Kakinuma A, Jaume JC, McLachlan SM, Rapoport B** 1997 Evidence that the thyrotropin receptor ectodomain contains not one, but two, cleavage sites. Endocrinology 138:2893–2899
3. **Wadsworth HL, Chazenbalk GD, Nagayama Y, Russo D, Rapoport B** 1990 An insertion in the human thyrotropin receptor critical for high affinity hormone binding. Science 249:1423–1425
4. **Smits G, Campillo M, Govaerts C, Janssens V, Richter C, Vassart G, Pardo L, Costagliola S** 2003 Glycoprotein hormone receptors: determinants in leucine-rich repeats responsible for ligand specificity. EMBO J 22:2692–2703
5. **Angelova K, de Jonge H, Granneman JC, Puett D, Bogerd J** 2010 Functional differences of invariant and highly conserved residues in the extracellular domain of the glycoprotein hormone receptors. J Biol Chem 285:34813–34827
6. **Costagliola S, Panneels V, Bonomi M, Koch J, Many MC, Smits G, Vassart G** 2002 Tyrosine sulfation is required for agonist recognition by glycoprotein hormone receptors. EMBO J 21:504–513
7. **Mueller S, Kleinau G, Jaeschke H, Paschke R, Krause G** 2008 Extended hormone binding site of the human thyroid stimulating hormone receptor: distinctive acidic residues in the hinge region are involved in bovine thyroid stimulating hormone binding and receptor activation. J Biol Chem 283:18048–18055
8. **Mueller S, Kleinau G, Szkudlinski MW, Jaeschke H, Krause G, Paschke R** 2009 The superagonistic activity of bovine thyroid-stimulating hormone (TSH) and the human TR1401 TSH analog is determined by specific amino acids in the hinge region of the human TSH receptor. J Biol Chem 284:16317–16324
9. **Fan QR, Hendrickson WA** 2005 Structure of human follicle-stimulating hormone in complex with its receptor. Nature 433:269–277
10. **Sanders J, Chirgadze DY, Sanders P, Baker S, Sullivan A, Bhardwaja A, Bolton J, Reeve M, Nakatake N, Evans M, Richards T, Powell M, Miguel RN, Blundell TL, Furmaniak J, Smith BR** 2007 Crystal structure of the TSH receptor in complex with a thyroid-stimulating autoantibody. Thyroid 17:395–410
11. **Grossmann M, Leitolf H, Weintraub BD, Szkudlinski MW** 1998 A rational design strategy for protein hormone superagonists. Nat Biotechnol 16:871–875
12. **Leitolf H, Tong KP, Grossmann M, Weintraub BD, Szkudlinski MW** 2000 Bioengineering of human thyrotropin superactive ana-

logs by site-directed "lysine-scanning" mutagenesis. Cooperative effects between peripheral loops. J Biol Chem 275:27457–27465
13. **East-Palmer J, Szkudlinski MW, Lee J, Thotakura NR, Weintraub BD** 1995 A novel, nonradioactive *in vivo* bioassay of thyrotropin (TSH). Thyroid 5:55–59
14. **Foti D, Russo D, Costante G, Filetti S** 1991 The biological activity of bovine and human thyrotropin is differently affected by trypsin treatment of human thyroid cells: thyroid-stimulating antibody is related to human thyrotropin. J Clin Endocrinol Metab 73:710–716
15. **Pierce JG, Parsons TF** 1981 Glycoprotein hormones: structure and function. Annu Rev Biochem 50:465–495
16. **Rapoport B, Takai NA, Filetti S** 1982 Evidence for species specificity in the interaction between thyrotropin and thyroid-stimulating immunoglobulin and their receptor in thyroid tissue. J Clin Endocrinol Metab 54:1059–1062
17. **Szkudlinski MW, Teh NG, Grossmann M, Tropea JE, Weintraub BD** 1996 Engineering human glycoprotein hormone superactive analogues. Nat Biotechnol 14:1257–1263
18. **Yamazaki K, Sato K, Shizume K, Kanaji Y, Ito Y, Obara T, Nakagawa T, Koizumi T, Nishimura R** 1995 Potent thyrotropic activity of human chorionic gonadotropin variants in terms of 125I incorporation and de novo synthesized thyroid hormone release in human thyroid follicles. J Clin Endocrinol Metab 80:473–479
19. **Wonerow P, Schöneberg T, Schultz G, Gudermann T, Paschke R** 1998 Deletions in the third intracellular loop of the thyrotropin receptor. A new mechanism for constitutive activation. J Biol Chem 273:7900–7905
20. **Swillens S** 1995 Interpretation of binding curves obtained with high receptor concentrations: practical aid for computer analysis. Mol Pharmacol 47:1197–1203
21. **Mueller S, Kleinau G, Jaeschke H, Neumann S, Krause G, Paschke R** 2006 Significance of ectodomain cysteine boxes 2 and 3 for the activation mechanism of the thyroid-stimulating hormone receptor. J Biol Chem 281:31638–31646
22. **Altschul SF, Gish W, Miller W, Myers EW, Lipman DJ** 1990 Basic local alignment search tool. J Mol Biol 215:403–410
23. **Chenna R, Sugawara H, Koike T, Lopez R, Gibson TJ, Higgins DG, Thompson JD** 2003 Multiple sequence alignment with the Clustal series of programs. Nucleic Acids Res 31:3497–3500
24. **Waterhouse AM, Procter JB, Martin DM, Clamp M, Barton GJ** 2009 Jalview version 2—a multiple sequence alignment editor and analysis workbench. Bioinformatics 25:1189–1191
25. **Kleinau G, Brehm M, Wiedemann U, Labudde D, Leser U, Krause G** 2007 Implications for molecular mechanisms of glycoprotein hormone receptors using a new sequence-structure-function analysis resource. Mol Endocrinol 21:574–580
26. **Farid NR, Szkudlinski MW** 2004 Minireview: structural and functional evolution of the thyrotropin receptor. Endocrinology 145:4048–4057
27. **Costagliola S, Swillens S, Niccoli P, Dumont JE, Vassart G, Ludgate M** 1992 Binding assay for thyrotropin receptor autoantibodies using the recombinant receptor protein. J Clin Endocrinol Metab 75:1540–1544
28. **Willey KP** 1999 An elusive role for glycosylation in the structure and function of reproductive hormones. Hum Reprod Update 5:330–355
29. **Chen CR, McLachlan SM, Rapoport B** 2011 Evidence that the thyroid-stimulating hormone (TSH) receptor transmembrane domain influences kinetics of TSH binding to the receptor ectodomain. J Biol Chem 286:6219–6224
30. **Bonomi M, Busnelli M, Persani L, Vassart G, Costagliola S** 2006 Structural differences in the hinge region of the glycoprotein hormone receptors: evidence from the sulfated tyrosine residues. Endocrinology 20:3351–3363
31. **Bruysters M, Verhoef-Post M, Themmen AP** 2008 Asp330 and Tyr331 in the C-terminal cysteine-rich region of the luteinizing hormone receptor are key residues in hormone-induced receptor activation. J Biol Chem 283:25821–25828
32. **Mizutori Y, Chen CR, McLachlan SM, Rapoport B** 2008 The thyrotropin receptor hinge region is not simply a scaffold for the leucine-rich domain but contributes to ligand binding and signal transduction. Mol Endocrinol 22:1171–1182
33. **Hamidi S, Chen CR, Mizutori-Sasai Y, McLachlan SM, Rapoport B** 2011 Relationship between thyrotropin receptor hinge region proteolytic posttranslational modification and receptor physiological function. Mol Endocrinol 25:184–194
34. **Szkudlinski MW, Fremont V, Ronin C, Weintraub BD** 2002 Thyroid-stimulating hormone and thyroid-stimulating hormone receptor structure-function relationships. Physiol Rev 82:473–502
35. **Szkudlinski MW** 2004 Past, presence and future of thyroid-stimulating hormone (TSH) superactive analogs. Cancer Treat Res 122:345–356
36. **Kosugi S, Mori T** 1996 Constitutive activation of the thyrotropin receptor by mutating CYS-636 in the sixth transmembrane segment. Biochem Biophys Res Commun 222:713–717
37. **Meyer EA, Castellano RK, Diederich F** 2003 Interactions with aromatic rings in chemical and biological recognition. Angew Chem Int Ed Engl 42:1210–1250
38. **Morris JC, Bergert ER, McCormick DJ** 1993 Structure-function studies of the human thyrotropin receptor. Inhibition of binding of labeled thyrotropin (TSH) by synthetic human TSH receptor peptides. J Biol Chem 268:10900–10905